ISBN: 978-3-95450-241-7 ISSN: 2673-5350 doi:10.18429/JACoW-IBIC2022-TH1I1

FIRST MEASUREMENT OF LONGITUDINAL PROFILE OF HIGH-POWER AND LOW-ENERGY H⁻ BEAM BY USING BUNCH SHAPE MONITOR WITH GRAPHITE TARGET

R. Kitamura* on behalf of J-PARC linac
JAEA/J-PARC, Tokai, Naka, Ibaraki, Japan

Abstract

A bunch-shape monitor (BSM) using the highly-oriented pyrolytic graphite (HOPG) target has been developed to measure the high-power and low-energy negative hydrogen ion beam at the front-end. The performance evaluation of the BSM using the HOPG target was conducted. The first measurement of longitudinal beam profiles at the front-end was demonstrated with the BSM. The measurement was consistent with the design simulation of the front-end. As a further application, the BSM using the HOPG target will be an attractive and powerful instrument to study the space-charge effect at the front-end.

INTRODUCTION

The Japan proton accelerator research complex (J-PARC) [1] linac supplies the 400-MeV negative hydrogen ion (H^-) beam to subsequent accelerators and experimental facilities. Recently, the user operation with a peak current of 50 mA was stable by the careful maintenance and beam tuning. Detailed beam studies are being conducted to reduce the beam loss towards higher power and the robustness of the stable operation. The medium-energy beam transport 1 (MEBT1) is important for the beam tuning of the linac. Figure 1 shows the configuration of the MEBT1. There are two functions of MEBT1 as follows. One is the beam matching between a 3-MeV radio-frequency quadrupole (RFQ) linac and a subsequent 50-MeV drift-tube linac. The other is the production of the bunch time structure for the injection into the rapid-cycle synchrotron. Since the parameters of the MEBT1 should be tuned to satisfy these requirements, the improvement of the longitudinal tuning in the MEBT1 is an interesting challenge to find a better solution for the high-power beam operation.

The bunch-shape monitor (BSM) [2,3] as the longitudinal beam profile monitor plays the important role to understand and improve the longitudinal beam dynamics in the MEBT1. However, the heat loading from the high-power and low-energy H^- beam in the MEBT1 caused the target failure of the BSM measurement which prevented the stable beam studies. We introduced the new graphite target for the BSM to mitigate the heat loading and successfully measured the longitudinal beam profiles in the MEBT1. In this report, the recent progress of the development of the BSM dedicated to the MEBT1 and its related studies are presented.

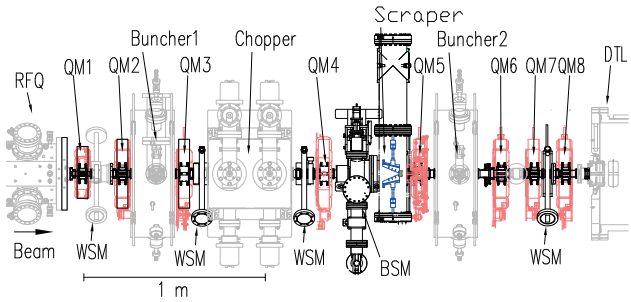

Figure 1: Configuration of the MEBT1.

NEW TARGETS FOR BSM

The BSM is a standard longitudinal beam profile monitor for the linac. Figure 2 shows the principle of the BSM. Secondary electrons are produced by the interaction between the H^- beam and the BSM target. The negative bias voltage is applied to the target to extract these secondary electrons into the deflector in the BSM. The electrons related to the longitudinal profile of the original H^- beam are modulated by the RF electric field in the deflector.

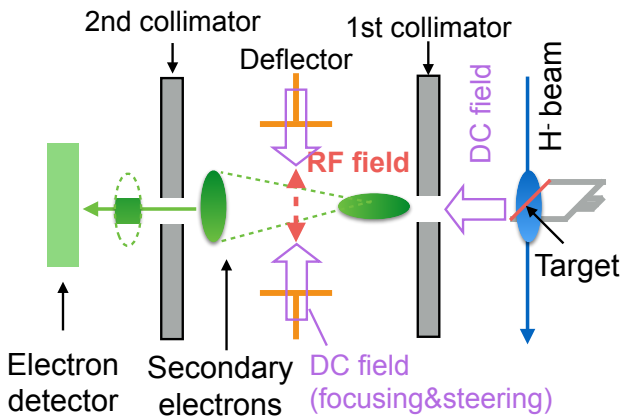

Figure 2: Principle of BSM.

The challenge of the BSM in the MEBT1 is to mitigate the heat loading from the high-power and the low-energy H^- beam. Therefore, we introduced a new strong target material for the BSM. There are three candidates for the BSM target as follows. One is the tungsten wire target, which is used as the standard target material for the usual BSM. However, the wire breaking frequently occurred due to heat loading in the MEBT1. Another candidate is a carbon nanotube (CNT)

* rkita@post.j-parc.jp

ISBN: 978-3-95450-241-7 ISSN: 2673-5350 doi:10.18429/JACoW-IBIC2022-TH1I1

wire [4, 5], which is used for the wire scanner monitor to measure the transverse profiles in the MEBT1. The advantage of the CNT is its low density. The effective heat loading to the target depends on the density of the target. The other candidate is the lamina graphite target. We used the highly-oriented pyrolytic graphite (HOPG) [6, 7] target, which is known as the candidate material of the beam scraper in the MEBT1. The advantage of the HOPG is its high thermal conductivity, which can reduce the thermal damage of the target.

Figure 3 shows the photographs of the CNT wire and the HOPG target mounted on the BSM target holder. Although the CNT is a good candidate for the BSM target, it is known as its electron emitter property. It is the disadvantage because the emission electrons cause the unexpected discharge of the bias voltage for the BSM target. Therefore, it should be confirmed whether the negative bias voltage is stably applied to the CNT wire. When the bias voltage was applied to the CNT wire, the luminescence from the insulator ceramics was observed. The spectrum peak due to emission electrons was detected by the spectroscopic measurement. As a result, the field electron emission from the CNT wire was inevitable and serious for the BSM operation.

On the other hand, the negative bias voltage was successfully applied to the HOPG target, which was a good characteristic as the BSM target. As described above, its high thermal conductivity is suitable to mitigate the heat loading from the high-power H^- beam. Therefore, we adopted the HOPG as the new target material of the BSM.

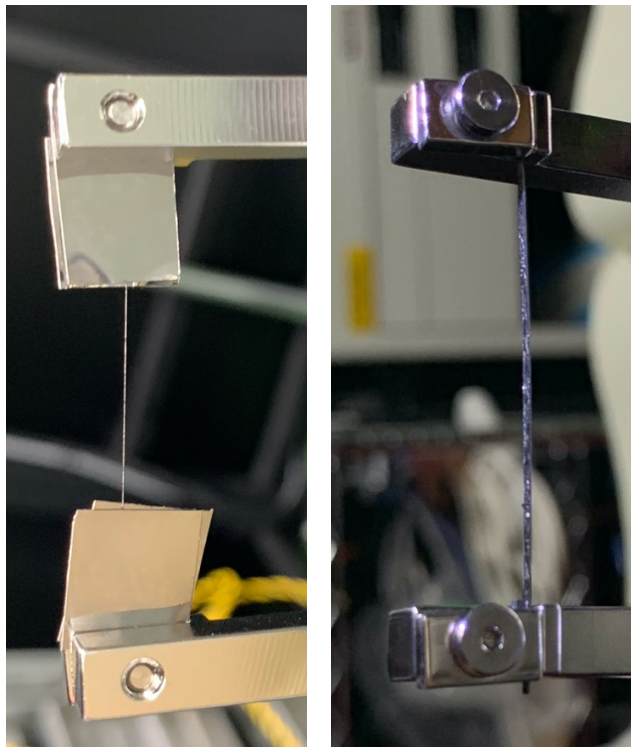

Figure 3: Photographs of the CNT wire (left) and HOPG (right) mounted on the BSM target holder. The diameter of the CNT wire is 0.1 mm and the size of the HOPG is a dimension of 0.2 mm(width)×1.0 mm(thickness)×48 mm(length).

STUDIES OF BSM USING GRAPHITE

The HOPG target is thicker than the original tungsten wire and the CNT wire. It should be confirmed whether the size of the HOPG target affects the measurement of the longitudinal profile. The test experiment was conducted at the test stand in the J-PARC linac building. The test stand consists of the 50-keV H^- ion source, the 3-MeV RFQ [8, 9], and the diagnostic beamline. The BSM was installed into the diagnostic beamline. Figure 4 shows the experimental setup of the test stand. The beam condition is as follows. The peak current, the energy, the pulse length, and repetition were 50 mA, 3 MeV, 50 μs, and 1 Hz, respectively, which was the almost same as the MEBT1.

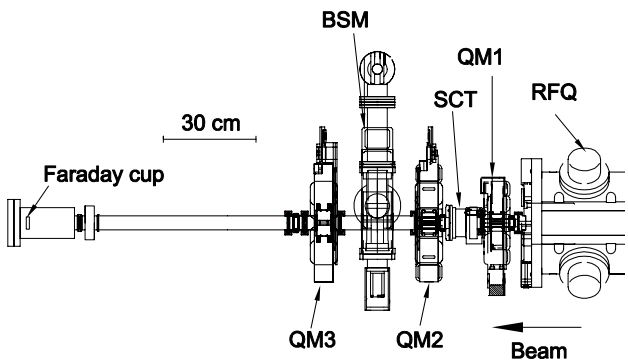

Figure 4: Configuration of the test stand.

Two types of HOPG targets were prepared, which were the small (0.2×1.0 mm^2) and the large (1.0×1.0 mm^2) targets. The minimum of the target size was determined by its cutting method (diamond wire sawing) [10]. The BSM target size affects the Time-of-Flight (ToF) of the extracted secondary electrons in the BSM. Therefore, it can be expected that the large target smears the longitudinal profile measured with the BSM. This ToF effect was estimated by the Geant4 simulation [11]. Figure 5 shows the comparison of longitudinal profiles measured with different sizes of HOPG targets. The profile corrected using the simulation was also shown in Fig. 5. Since the corrected profile with the target size of 0.2×1.0 mm^2 was consistent with the profile measured with that of 1.0×1.0 mm^2, we confirmed that the ToF effect could be evaluated with this procedure.

One advantage of the BSM using the HOPG target (HOPG-BSM) is to measure the longitudinal profile at any horizontal position. This implies the HOPG-BSM is not only the longitudinal profile monitor but also the both longitudinal and transverse profile monitor. In the first trial, we demonstrated the observation of the correlation between the longitudinal and transverse profiles under the space-charge effect. Figure 6 shows the longitudinal and horizontal profiles measured with the BSM when the quadrupole magnet was turned on and off. When the space-charge effect affects the beam profile, for example, it is expected that

ISBN: 978-3-95450-241-7 ISSN: 2673-5350 doi:10.18429/JACoW-IBIC2022-TH1I1

the transverse focusing affects longitudinal profile through space-charge force. From Fig. 6, we observed the correlation between the longitudinal phase and horizontal bunch profile. Although detailed studies are necessary, this result is attractive to understand the behavior of the high-power H^- beam at the front-end.

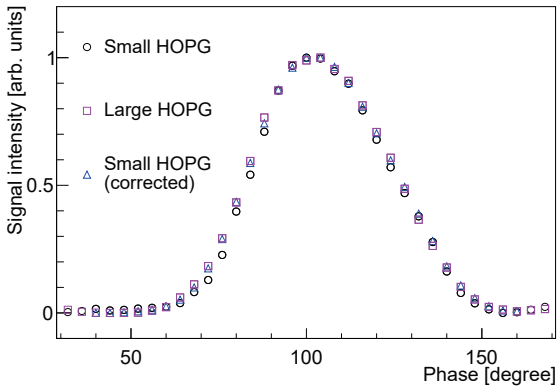

Figure 5: Comparison of longitudinal profiles measured with different size of HOPG targets.

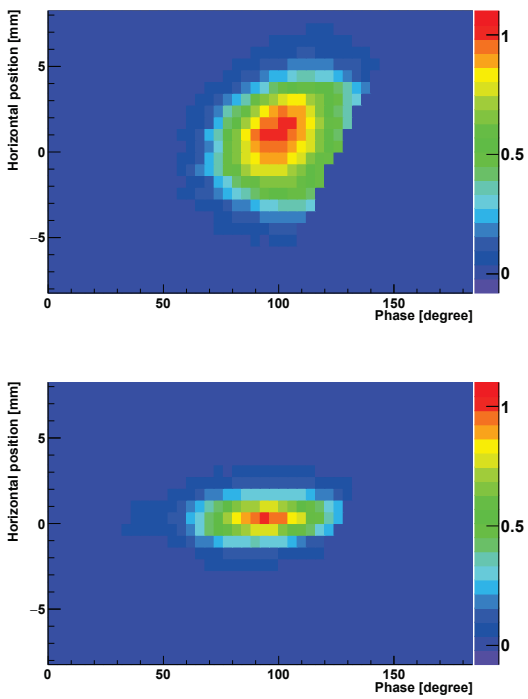

Figure 6: Longitudinal and horizontal profiles measured with the BSM. the top figure shows the profile tuning off the quadrupole magnet and the bottom figure shows that turning on the magnet.

FIRST LONGITUDINAL MEASUREMENT

The first measurement of the longitudinal beam profile in the MEBT1 was demonstrated with the HOPG-BSM. The peak current, the energy, the pulse length, and repetition in the measurement were 50 mA, 3 MeV, 100 µs, and 1 Hz, respectively. The longitudinal amplitude-scan method [12] with the buncher cavity was used to evaluate longitudinal beam parameters. The stable longitudinal measurement was realized thanks to the HOPG target. Figure 7 shows the typical waveform measured with the BSM. No target failure occurred during the measurement.

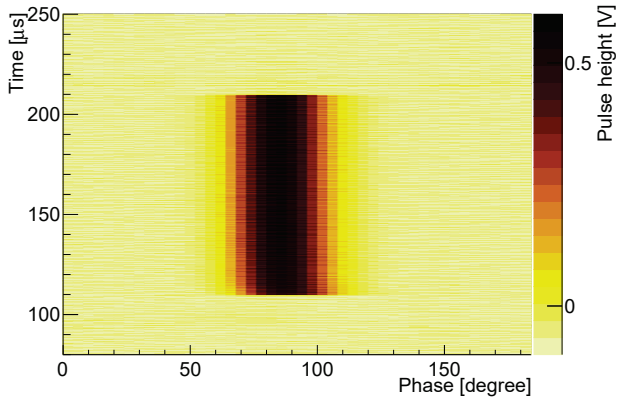

Figure 7: Measured waveform of the BSM.

Longitudinal beam parameters were evaluated using the IMPACT [13], which is the Particle-In-Cell code, to consider the space-charge effect in the MEBT1. Figure 8 shows the longitudinal bunch width measured with the BSM in terms of the buncher voltage. The data was used for the fitting of the IMPACT simulation. The fitting curve was consistent with the measurement for the amplitude scan.

Initial Twiss parameters at the RFQ exit evaluated with the data and the IMPACT were compared with the design simulation for the H^- ion source and the RFQ. Figure 9 shows longitudinal ellipses measured with the BSM and the design ellipse at the RFQ exit. The measurement using the BSM was consistent with the design simulation. This result shows our BSM and MEBT1 system were well understood in the high-power operation.

SUMMARY

The BSM using the HOPG target has been developed to measure the high-power H^- beam in the MEBT1. In this study, the performance evaluation of the HOPG-BSM was conducted. The first measurement of the longitudinal beam profile was demonstrated using the BSM in the MEBT1. The measurement was consistent with the design simulation of the MEBT1. Our HOPG-BSM is the attractive instrument and plays the important role to study the space-charge effect at the front-end.

ISBN: 978-3-95450-241-7 ISSN: 2673-5350 doi:10.18429/JACoW-IBIC2022-TH1I1

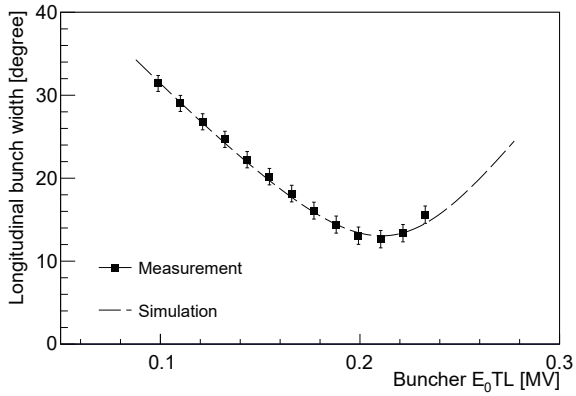

Figure 8: Longitudinal bunch width measured with the BSM in terms of the buncher voltage.

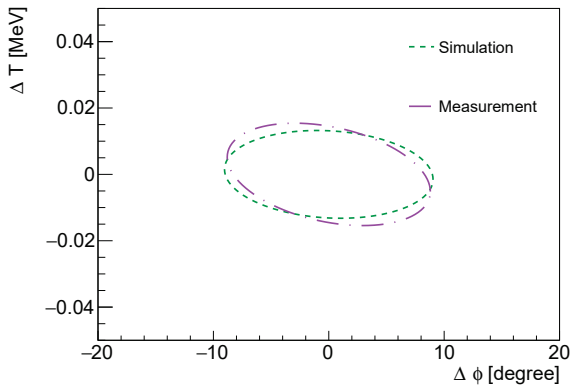

Figure 9: Longitudinal ellipses measured with the BSM and the design ellipse at the RFQ exit.

REFERENCES

[1] K. Hasegawa *et al.*, "Performance and Status of the J-PARC Accelerators", in *Proc. IPAC'18*, Vancouver, Canada, Apr.-May 2018, pp. 1038–1040. doi:10.18429/JACoW-IPAC2018-TUPAL017

[2] A. V. Feschenko, "Methods and Instrumentation for Bunch Shape Measurements (Invited)", in *Proc. PAC'01*, Chicago, IL, USA, Jun. 2001, paper ROAB002, pp.517–521.

[3] R. Kitamura *et al.*,"Bunch-Size Measurement of the High-Intensity H- Beam with 3 MeV by the Bunch Shape Monitor", *JPS Conf. Proc.*, vol. 33, p. 011012, 2021. doi:10.7566/JPSCP.33.011012

[4] A. Miura, T. Miyao, and K. Moriya, "Application of carbon nanotube wire for beam profile measurement of negative hydrogen ion beam", *J. Phys.: Conf. Ser.*, vol. 1067, p. 072020, 2018. doi:10.1088/1742-6596/1067/7/072020

[5] R. Kitamura *et al.*, "Development of the Bunch Shape Monitor Using the Carbon-Nano Tube Wire", in *Proc. IPAC'19*, Melbourne, Australia, May 2019, pp. 2543–2546. doi:10.18429/JACoW-IPAC2019-WEPGW033

[6] Y. Yamada, M. Yanase, D. Miura, and K. Chikuba, "Novel heatsink for power semiconductor module using high thermal conductivity graphite", *Microelectron. Reliab.*, vol. 64, pp. 484–488, 2016. doi:10.1016/j.microrel.2016.07.029

[7] L. Li, A. Fukui, and A. Wakejima, "Bonding GaN on high thermal conductivity graphite composite with adequate interfacial thermal conductance for high power electronics applications", *Appl. Phys. Lett.*, vol. 116, p. 142105, 2020. doi:10.1063/1.5144024

[8] Y. Kondo, T. Morishita, and R. A. Jameson, "Development of a radio frequency quadrupole linac implemented with the equipartitioning beam dynamics scheme", *Phys. Rev. Accel. Beams*, vol. 22, p. 120101, 2019. doi:10.1103/PhysRevAccelBeams.22.120101

[9] T. Morishita and Y. Kondo, "Electromagnetic design and tuning of the four-vane radio frequency quadrupole with nonuniform intervane voltage profile", *Phys. Rev. Accel. Beams*, vol. 23, p. 111003, 2020. doi:10.1103/PhysRevAccelBeams.23.111003

[10] A. Kumar and S. N. Melkote, "Diamond Wire Sawing of Solar Silicon Wafers: A Sustainable Manufacturing Alternative to Loose Abrasive Slurry Sawing", *Procedia Manuf.*, vol. 21, pp. 549–566, 2018. doi:10.1016/j.promfg.2018.02.156

[11] Geant4, http://geant4.cern.ch

[12] H. Wiedemann, *Particle Accelerator Physics 4th Edition*, Springer, 2015, pp.222–227.

[13] J. Qiang, R. D. Ryne, S. Habib, and V. Decyk, "An Object-Oriented Parallel Particle-in-Cell Code for Beam Dynamics Simulation in Linear Accelerators", *J. Comput. Phys.*, vol. 163, pp. 434–451, 2000. doi:10.1006/jcph.2000.6570